APPLICATION OF POLARIMETRIC SAR TO EARTH REMOTE SENSING

Jakob J. van Zyl and Yunjin Kim

Jet Propulsion Laboratory

California Institute of Technology

Pasadena, CA U.S.A. 91109

1. INTRODUCTION

Electromagnetic scattering is fundamentally a vector process. Therefore, to capture all the information from the scattered waves, the full polarization vector of the waves received by the radar should be measured. Polarimetric SARs were first demonstrated in the early 1980s, and made their debut in space with the SIR-C/X-SAR mission in 1994. By the end of the 1990's several polarimetric airborne SAR systems were operating in the United States, Europe and Japan. As of the writing of this paper, both the German TerraSAR-X (X-band) and the Japanese ALOS PALSAR (L-Band) space missions offer fully polarimetric data in experimental models. This paper will provide an overview of the application of polarimetric SAR data to Earth remote sensing. Here we will illustrate only few of the topics that will be covered.

2. POLARIZATION SIGNATURES – A NEW PERSPECTIVE

Polarization signatures [1-4] have become a standard way to visualize the information in polarimetric scattering. The standard polarization signature plots the received power as a three-dimensional figure where the two horizontal axes denote the polarization orientation and ellipticity of the transmitted wave, respectively, and the strength of the received power is displayed in the vertical offset from the horizontal plane. Often only the signature displaying the so-called co-polarized power, *i.e.* the case where identical polarizations are used for transmission and reception of the waves, is displayed. Sometimes, however, both co-and cross-polarized (orthogonally polarized antennes used for transmission and reception) signatures are displayed.

A new, and potentially more insightful, way of displaying these figures is introduced in [4]. In this display, the Poincare sphere axes are used to denote the polarization of the transmitted wave, and the

strength of the receive power is displayed as the distance from the origin of the Poincare sphere for a given polarization. Figure 1 shows the definition of the two types of signatures. Figure 2 shows the power of the new 3-D signatures to visualize scattering matrices that represent orthogonal scattering processes.

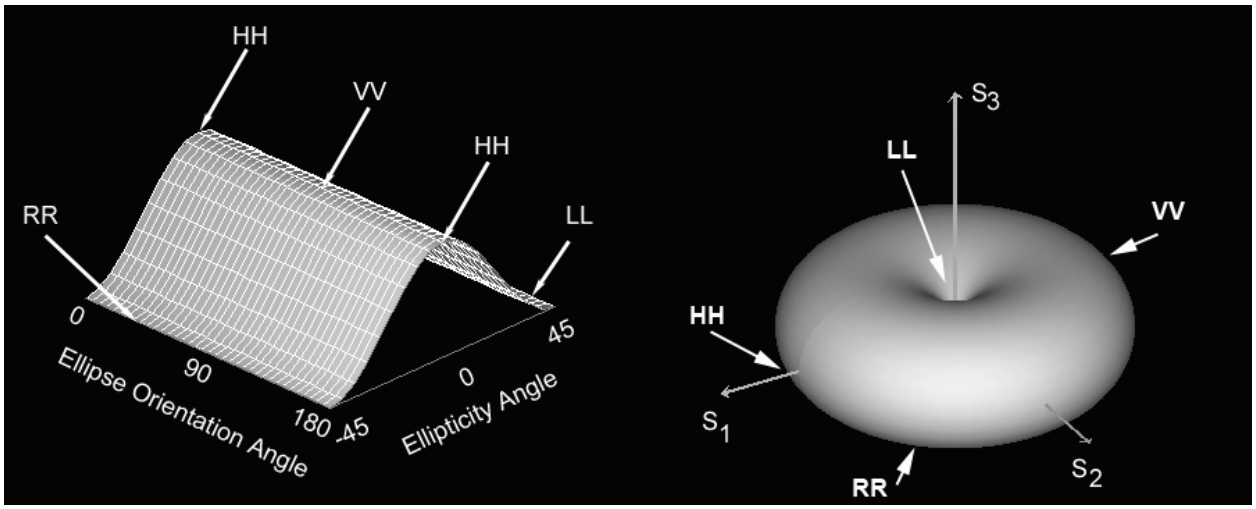

Fig. 1. Standard (Left) and new 3-D (Right) co-polarization signatures of a trihedral corner reflector.

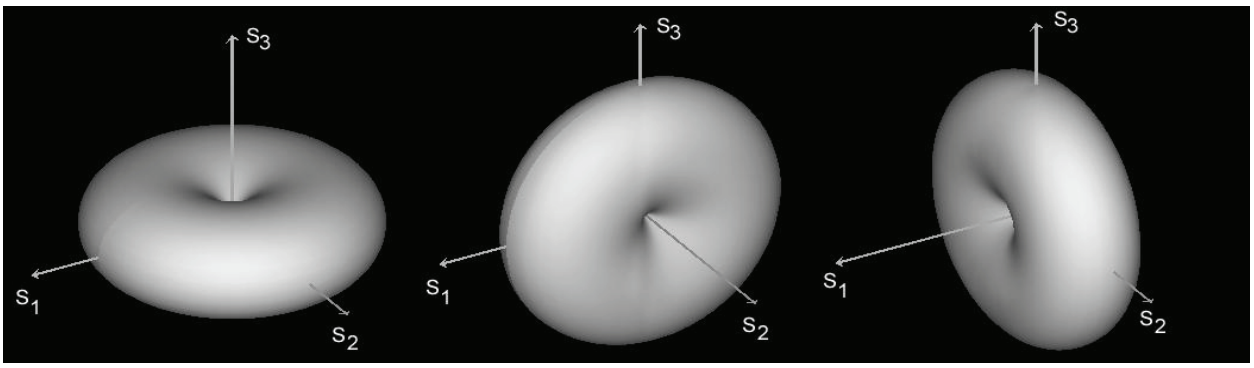

Fig. 2. Polarization responses of three scatterers: trihedral corner reflector (left), dihedral corner reflector (middle) and dihedral corner reflector rotated by 45 degrees (right). The scattering matrices of these three scatterers are orthogonal and represent eigenvectors in the Pauli basis. The three signatures are identical, but rotated by 90 degrees relative to each other.

3. MODEL-BASED DECOMPOSITION OF SCATTERING

Several groups have proposed ways in which to decompose polarimetric scattering into simpler scattering mechanisms. Van Zyl *et al* [5] showed that some of the more commonly used decompositions suffer from a fatal flaw: they often result in negative powers assigned to some of the scattering mechanisms.

They go on to show that a simple check would be to constrain the model based decomposition by insisting that for every decomposition step, the remaining covariance matrix must have non-negative eigenvalues. For example, we can write the decomposition in the form

$$\langle [\mathbf{C}] \rangle = a[\mathbf{C}_{model}] + [\mathbf{C}_{remainder}] \quad (1)$$

Here, the matrix on the left represents the measured covariance matrix and first term on the right represents the covariance matrix predicted by some model such as randomly oriented branches. Recognizing that the form of this covariance matrix may be different from the measured matrix, they add the second term, which will contain whatever is in the measured matrix that is not consistent with the model matrix. They then determine the value of a to be the largest value that still ensures that the second matrix on the left will have non-negative eigenvalues

Figure 3 compares the results of the constrained non-negative eigenvalue decomposition to that of the popular three-component model introduced by Freeman and Durden [6]. It is shown in [4] that the Freeman-Durden decomposition over-estimates the vegetation contribution by 10-20%.

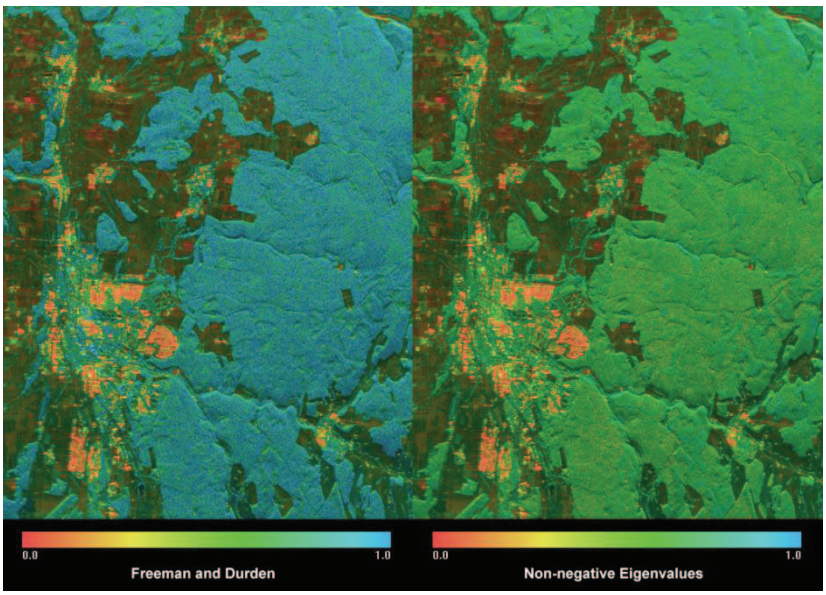

Fig. 3. These images display the fraction of the observed total power that can be attributed to scattering from a uniformly randomly oriented layer of cylinders. The image on the left follows the calculation proposed by Freeman and Durden [10], while the image on the right is calculated by requiring that the remaining eigenvalues not be negative. On the average the image on the right shows about 10-20% lower values for the forested areas than the one on the left.

ACKNOWLEDGEMENT

This work was performed at the Jet Propulsion Laboratory, Claifornia Institute of Technology, under a contract with the National Aeronautics and Space Administration (NASA).

REFERENCES

[1] van Zyl, J.J., *On the Importance of Polarization in Radar Scattering Problems*, Ph.D. Thesis, Caltech Antenna Laboratory Report No. 120, California Institute of Technology, Pasadena, CA, 1985.

[2] van Zyl, J.J., H.A. Zebker and C. Elachi, "Imaging radar polarization signatures: Theory and observation," *Radio Science*, **22**, 529-543, 1987.

[3] Zebker, H.A., J.J. van Zyl, and D.N. Held, "Imaging Radar Polarimetry from Wave Synthesis," *J. Geophys. Res.,* **92**, pp. 683-701, 1987.

[4] van Zyl, J.J. and Y. Kim, *Synthetic Aperture Radar Polarimetry,* In Press, Wiley and Sons, New York, 2010.

[5] van Zyl, J.J., M. Arii, and Y. Kim, "Model-based decomposition of polarimetric SAR covariance matrices constrained for non-negative eigenvalues," submitted to *IEEE Transactions on Geoscience and Remote Sensing*, 2009.

[6] A. Freeman and S. Durden, "A three component scattering model for polarimetric SAR data," *IEEE Transactions on Geoscience and Remote Sensing,* **GE-36,** No 3, pp. 963-973, 1998.